Research Paper

EARTHQUAKE SPECTRA

Novel approach for energy-spectrum-based probabilistic seismic hazard analysis in regions with limited strong earthquake data

Earthquake Spectra
1–20

DOI: 10.1177/87552930241263621
journals.sagepub.com/home/eqs
Sage

Haizhong Zhang[1], Rui Zhang[2], and Yan-Gang Zhao[3]

Abstract

With the rapid development of energy-based seismic design, probabilistic seismic hazard analysis (PSHA) in terms of the input energy spectrum, E_I, has become increasingly important. Generally, implementing E_I-based PSHA requires a ground-motion prediction equation (GMPE) for E_I. However, although a GMPE for E_I can be constructed in regions with abundant earthquake data based on regression analyses, it is difficult to obtain in regions lacking strong ground-motion records. Therefore, this study proposes a new approach for performing E_I-based PSHA in regions with limited earthquake data. Instead of using a GMPE for E_I directly, a model of Fourier amplitude spectrum (FAS) is adopted, which can be determined using a small number of earthquake data with small-to-moderate magnitudes. Then, the E_I of the ground motion is obtained from FAS based on the relationship between E_I and FAS. Furthermore, to calculate the annual intensity exceedance rate within the proposed framework of adopting the FAS model, a highly efficient method, namely, the moment method, is applied. Several numerical examples indicate that the proposed approach not only is suitable for regions lacking strong ground-motion records but also performs very efficiently in calculating the annual intensity exceedance rate.

Keywords

Energy-based seismic design, probabilistic seismic hazard analysis, input energy spectrum, Fourier amplitude spectrum, moment method

Date received: 23 September 2023; accepted: 31 May 2024

[1]Eco-Science, Faculty of Agriculture, Yamagata University, Tsuruoka, Japan
[2]School of Geography and Tourism, Qilu Normal University, Jinan, China
[3]Key Laboratory of Urban Security and Disaster Engineering of Ministry of Education, Beijing University of Technology, Beijing, China

Corresponding author:
Yan-Gang Zhao, Key Laboratory of Urban Security and Disaster Engineering of Ministry of Education, Beijing University of Technology, Beijing 100124, China.
Email: zhaoyg@bjut.edu.cn

Introduction

Since the introduction of the energy concept in structural seismic designs by Housner (1956), energy-based seismic design has become increasingly popular and has attracted the attention of many researchers (Akiyama, 1985; Akiyama et al., 1993; Decanini and Mollaioli, 1998, 2001; Kunnath and Chai, 2004; Kuwamura and Galambos, 1989; Vahdani et al., 2019; Zhang et al., 2023a, 2023b). The energy-based seismic design is advantageous over the traditional force- or displacement-based seismic design, because it quantifies not only the maximum strength or displacement but also the cumulative hysteretic behavior of structures. The basic rule of the energy-based seismic design is to keep the energy dissipation capacity of the structure larger than the earthquake energy demand. Therefore, to perform an energy-based seismic design, it not only needs to estimate the energy dissipation capacity of the structure but also needs to determine the earthquake energy demand.

The hysteretic energy spectrum, E_H, representing the energy dissipated by the cumulative plastic deformation of a single-degree-of-freedom (SDOF) structure, is typically used to characterize the earthquake energy demand for the energy-based seismic design. The reason for using E_H is that the energy dissipated through the cumulative plastic deformation truly contributes to the cumulative damage. The other portion of the earthquake energy imparted into the structure, which is dissipated by the structural damping, does not make a contribution to the cumulative damage. Nevertheless, many studies (Chai and Fajfar, 2000; Chapman, 1999; Du et al., 2020; Kuwamura and Galambos, 1989) prefer to first determine the input energy spectrum, E_I, representing the total earthquake energy imparted into an SDOF structure, and then obtain E_H based on a hysteretic-to-input energy ratio spectrum E_H/E_I. Because the E_I is a more stable quantity determined primarily by the ground motion as well as structural period and mass, and is typically uncoupled with the energy dissipation capacity of the structure. Moreover, the E_I is commonly expressed in terms of the energy equivalent velocity spectrum, V_{eq}, ($V_{eq} = (2E_I/m)^{0.5}$) to eliminate the effect of the structural mass m.

Similar to traditional ground-motion-intensity measures, for example, response spectra, to determine the intensity of the V_{eq} used for the energy-based seismic design, two approaches are available: deterministic seismic hazard analysis (DSHA) or probabilistic seismic hazard analysis (PSHA). DSHA is suitable when it is easy to identify the largest controlling earthquake source from various sources capable of producing damaging ground motions. Otherwise, it is advisable to use PSHA and take into account all earthquake sources capable of producing damaging ground motions (Baker, 2008). The performance of the PSHA requires a ground-motion prediction equation (GMPE) for V_{eq} to estimate the V_{eq} intensity on a site of interest caused by a specific earthquake source. In principle, the GMPE for V_{eq} can be derived by performing regression analysis over a database of earthquake records at different sites in the considered region (Alıcı and Sucuoğlu, 2016, 2018; Chapman, 1999; Cheng et al., 2014, 2020; Chou and Uang, 2000; Gong and Xie, 2005). However, many regions in the world, particularly the intra-plate regions across the globe, have a paucity of recorded data although they are seismically active, and it is difficult to generate reasonable GMPEs in these regions. Some studies (Tselentis et al., 2010) directly used GMPEs for V_{eq} from some other data-rich regions to perform a PSHA in such regions. However, the selection of a specific GMPE from another region carries a strong subjectivity aspect for the hazard analyst. More importantly, neglecting regional seismological differences can often lead to an unrealistic estimation of ground motion (Bora et al., 2014, 2015, 2016).

This study aims to develop a new approach for performing the V_{eq}-based PSHA in regions with limited ground-motion records. Specifically, in contrast to directly using a GMPE for V_{eq}, a model of Fourier amplitude spectrum (FAS) is adopted. Since the transmission of FAS is fully consistent with linear system theory (Bora et al., 2014, 2015, 2016), the FAS model can be determined using a relatively small number of seismic records with small-to-moderate magnitudes (Boore, 2018, 2020). Then, the V_{eq} of the ground motion is obtained based on the relationship between V_{eq} and FAS. Subsequently, to calculate the annual intensity exceedance rate within the proposed framework of adopting the FAS model, a highly efficient method, namely, the moment method, is applied. The rest of this paper is organized as follows. First, the FAS model and the method to estimate the ground-motion V_{eq} based on the relationship between V_{eq} and FAS are introduced. Then, an efficient method, namely, the moment method, to calculate the annual intensity exceedance rate is presented. Subsequently, some numerical examples applying the proposed approach are conducted and compared with applying the traditional GMPE-based approach. Finally, the conclusions of this study are summarized.

Estimation of the input energy spectrum based on a Fourier amplitude spectral model

To perform a V_{eq}-based PSHA in regions with a paucity of seismic records, it needs to estimate V_{eq} of ground motion on a site of interest from a specific earthquake source. For this purpose, it is easy to think of adopting a GMPE of V_{eq} obtained in data-rich regions. However, since the GMPE for V_{eq} can vary significantly in different regions due to regional seismological differences, the application of GMPE for V_{eq} from other regions may lead to unreasonable results. Therefore, it needs to find another approach to estimate the V_{eq} of ground motion suitable for regions lacking seismic records. Since the transmission of FAS is fully consistent with linear system theory (Bora et al., 2014, 2015, 2016), an FAS model can be determined using a relatively small number of seismic records with small-to-moderate magnitudes (Boore, 2018, 2020). Therefore, in contrast to directly using a GMPE of V_{eq}, an FAS model is adopted, and the V_{eq} of the ground motion is obtained based on the relationship between V_{eq} and FAS.

Estimation of input energy spectrum

This section presents a method for estimating the E_I of the ground motion based on an FAS model whose parameters can be determined using a small number of seismic records (Boore, 2018, 2020). There are various FAS models; the simplest method involves using seismology theory to compute the radiated FAS from a point source in terms of the various source, path, and site parameters. This study utilizes the seismological point-source theory to derive the FAS based on the description of Boore (2003). The point-source FAS of the ground-motion acceleration, $Y(f)$ (cm/s), is expressed as

$$Y(f) = [0.78\frac{\pi}{\rho\beta^3}M_0\frac{f^2}{1+(f/f_c)^2}][Z(R)\times\exp(\frac{-\pi fR}{Q(f)\beta})][exp(-\pi\kappa_0 f)A(f)] \quad (1)$$

where f is the frequency (Hz); ρ is the mass density of the crust (g/cm^3); β is the shear-wave velocity of the crust (km/s); R is the distance from the source (km); $Z(R)$ is the geometric attenuation; κ_0 is the site diminution (s); $Q(f)$ is the anelastic attenuation; $A(f)$ is the crust amplification; M_0 is the seismic moment (dyne cm), which is related to the moment magnitude, M, as $M_0 = 10^{1.5(M + 10.7)}$; f_c is the corner frequency given as $f_c = 4.9 \times 10^6 \beta(\Delta\sigma/M_0)^{1/3}$; and $\Delta\sigma$ is the stress drop (bars). This FAS model has been thoroughly investigated and verified using real seismic records (Atkinson and Boore, 2014; Boore, 2003) and has been extensively used by numerous studies (Kottke and Rathje, 2013; Rathje and Ozbey, 2006; Wang and Rathje, 2016; Zhang et al., 2023c; Zhang and Zhao, 2020, 2021, 2022; Zhao et al., 2023).

The values of these seismological parameters ($\Delta\sigma$, κ_0, $Z(R)$, $Q(f)$, etc.) needed in Equation 1 vary across different regions; they can be determined based on limited earthquake data recorded in the specific area of practical application (Boore et al., 2010; Boore and Thompson, 2015). In the study of Boore (2015), the stress drop $\Delta\sigma$ was derived from the inversion of an orientation-independent response spectra RotD_{50}, as defined by Boore (2010). Consequently, the corresponding FAS obtained by Equation 1 is compatible with the RotD_{50} response spectrum. Goulet et al. (2018) also defined an orientation-independent FAS. However, since this study focuses on the estimation of V_{eq}, the stress drop $\Delta\sigma$ should be derived to match an orientation-independent V_{eq}. Given that most current studies use the geometric mean of the two horizontal ground motion components (Alıcı and Sucuoğlu, 2016, 2018), to be compatible with current studies, the stress parameter $\Delta\sigma$ should be derived from the inversion of the geometric mean V_{eq}.

To incorporate rupture characteristics, which are particularly necessary for large-magnitude earthquakes, stochastic finite-fault modeling can be employed in principle. Applying the finite-fault model, a large fault can be subdivided into multiple subfaults (Beresnev and Atkinson, 1998), and the ground motions originating from each of these subfaults are computed using the point-source method and subsequently aggregated at the observation point. Nevertheless, it is more convenient to capture the essential aspects of motions from a finite fault in a single point-source simulation by the use of an appropriate point-source distance, R_{ps}. Boore (2009) introduced an effective point-source distance, R_{EFF}, to modify the source-to-site distance R. The R_{EFF} has the disadvantage that it is based on a specific source and site geometry. A more general version of R_{ps} has been proposed by Boore and Thompson (2015) and is expressed as

$$R_{\text{PS}} = \sqrt{R_{\text{RUP}}^2 + h^2} \tag{2}$$

where R_{RUP} is the rupture distance, and h is a finite-fault factor expressed as

$$\log(h(M)) = \begin{cases} a_1 + b_1(M - M_{t1}) & M \leqslant M_{t1} \\ c_0 + c_1(M - M_{t1}) + c_2(M - M_{t1})^2 + c_3(M - M_{t1})^3 & M_{t1} < M < M_{t2} \\ a_2 + b_2(M - M_{t2}) & M \geqslant M_{t2} \end{cases} \tag{3}$$

In Equation 3, a_1, a_2, b_1, b_2, c_0–c_3, M_{t1}, and M_{t2} are coefficients that have been given in Table 1 of Boore and Thompson (2015).

In addition, many studies have developed GMPEs for FAS in regions with both limited and abundant earthquake data (Bayless and Abrahamson, 2018; Lavrentiadis et al., 2023). Furthermore, Lavrentiadis and Abrahamson (2023) applied the FAS GMPE to construct a GMPE for the response spectrum based on random vibration theory. In cases where a nonergodic GMPE for FAS, such as the one of Lavrentiadis et al. (2023), has been well constructed for the region of interest, it's also feasible to utilize the FAS GMPE instead of the aforementioned FAS model in this study. However, in regions without nonergodic

Table 1. Information of probability density functions for the considered random variables

Parameter	Type of distribution	Mean value	Coefficient of variation
Density of crust ρ (g/cm^3)	lognormal	2.8	30%
Stress drop $\Delta\sigma$ (bar)	lognormal	400	30%
Shear-wave velocity of crust β (km/s)	lognormal	3.7	30%
Site diminution κ_0 (s)	lognormal	0.04	30%

FAS GMPEs, using an FAS model may be more convenient for regions with limited earthquake data. Because determining an FAS model requires significantly fewer earthquake data and efforts compared to the construction of a GMPE for FAS. For example, Boore (2015) determined the parameters of the FAS model only using eight earthquakes.

Then, to obtain E_I of the ground motion from the FAS model, an equation connecting the FAS and E_I is desirable. Two previous studies have theoretically discussed the relationship between the FAS and E_I. Kuwamura et al. (1994) found that E_I can be estimated with a smoothed version of the FAS. Subsequently, Ordaz et al. (2003) derived a more explicit and simple expression for estimating the E_I from the FAS, which is expressed as,

$$\frac{E_I(\bar{\omega},\xi)}{m} = -\frac{1}{\pi}\int_0^\infty |Y(\omega)|^2 Re[Hv(\bar{\omega},\omega,\xi)]d\omega \tag{4 − 1}$$

where ω is the circular frequency of the FAS ($\omega = 2\pi f$), $\bar{\omega}$ is the circular frequency of a single-degree-of-freedom (SDOF) oscillator, and ξ is the oscillator damping ratio. $Hv(\bar{\omega},\omega,\xi)$ is the oscillator transfer function of the ground acceleration to the relative velocity, which is a complex number. Its real part can be expressed as,

$$Re[Hv(\bar{\omega},\omega,\xi)] = -\frac{2\xi\bar{\omega}\omega^2}{(\bar{\omega}^2-\omega^2)^2+(2\xi\omega\bar{\omega})^2} \tag{4 − 2}$$

To eliminate the dependence on mass m, the input energy spectrum E_I can be converted into the equivalent input energy velocity, V_{eq}, via the following expression:

$$V_{eq}(\bar{\omega},\xi) = \sqrt{\frac{2E_I(\bar{\omega},\xi)}{m}} \tag{5}$$

Hence, using Equations 1–5, the ground-motion E_I and V_{eq} can be obtained from an earthquake source in terms of the various source, path, and site parameters. In addition, it is important to note that another advantage of using FAS to derive E_I and V_{eq} is the possibility to obtain results for multiple damping ratios in a straightforward manner. This is an advantage that the GMPE for V_{eq} lacks, as it is usually developed for a specific damping ratio. Results relating to this point will be shown in the following section.

Comparison with time-series analysis

To confirm the accuracy of the proposed method for estimating V_{eq} based on the FAS model, the V_{eq} values were calculated using Equations 1–5 and compared with those calculated using traditional time-series analysis. To this end, a wide range of oscillator periods T_0 ($T_0 = 1/f$) (0.01–10 s), damping ratios ξ (5%–50%), moment magnitude M (4-8), and rupture distance R_{RUP} (20–200 km) were considered. The values of the seismological parameters required in Equation 1 for central and eastern North America (CENA) are used in this section and are determined according to Boore and Thompson (2015). The reason for selecting CENA for comparative analyses is that the seismological parameters of CENA were relatively well studied. The parameters are taken from Table 1 of Wang and Rathje (2016). For each FAS obtained using Equation 1 and considering a pair of M and R_{RUP}, a suite of 100 time-series signals was generated using SMSIM (Boore, 2005) considering the finite-fault effects. Then, the E_I values for the generated time series were calculated based on its definition in the time-series domain, which is expressed as

$$E_I = -\int_0^t m\ddot{x}_g \dot{x} dt \tag{6}$$

where $\ddot{x}_g$ is the generated time-series acceleration, $\dot{x}$ is the corresponding velocity response of the SDOF oscillator, t is time, and its value corresponds to the end of the ground motion duration. The oscillator-response velocity $\dot{x}$ is calculated based on the direct integration method of Nigam and Jennings (1969). The comparisons of the average values of V_{eq} for the generated time series with those calculated by Equations 1–5 are shown in Figures 1 and 2. It can be found that the V_{eq} values obtained using the proposed method agree very well with those acquired from the time-series analysis. It can also be found that the proposed method can directly predict the V_{eq} values for multiple damping ratios.

Furthermore, the V_{eq} values derived from Equations 1–5 are compared with those calculated using seismic ground motions recorded in CENA from the Pacific Earthquake Engineering Research Center database. Seismic records were selected with a magnitude larger than 5 and rupture distance less than 300 km, which are generally of interest in earthquake engineering. Some representative results are shown in Figure 3. Overall, the V_{eq} values obtained using the proposed method also agree well with those calculated using real seismic records.

Annual intensity exceedance rate based on the moment method

To obtain the intensity of a V_{eq} corresponding to a certain return period based on PSHA, it needs to calculate the probability that V_{eq} exceeds a specified intensity at a given site during a specified time period, and considering all the earthquake sources capable of producing damaging ground motions. If the occurrence of seismic events is assumed to follow a homogeneous stochastic Poisson process, once the annual rate exceeding a specific intensity for each considered earthquake source is known, the exceedance probability at a site during a specified time period considering all sources can be easily obtained. In theory, the annual intensity exceedance rate, $V(im)$, of a source is estimated by,

$$\begin{aligned} V(im) &= \nu P(IM > im) \\ &= \nu \int_M \int_R \int_{X_3} \cdots \int_{X_n} P(IM > im | M, R, X_3, \cdots, X_n) f_M(m) f_R(r) f_{X_3}(x_3) \cdots f_{X_n}(x_n) dm dr dx_3 \cdots dx_n \end{aligned} \tag{7}$$

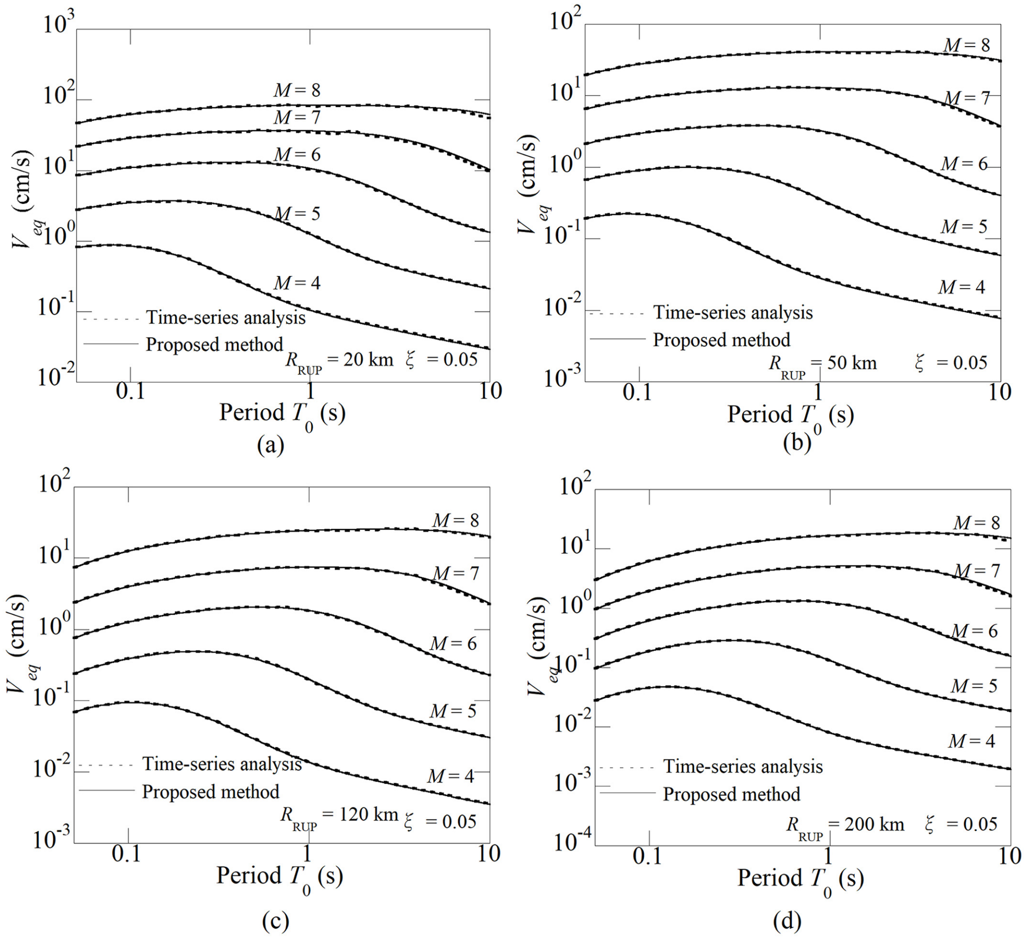

Figure 1. Comparison of V_{eq} results calculated by the proposed method and time-series analysis for a 5% damping ratio considering different moment magnitude M with the rupture distance R_{RUP} being: (a) R_{RUP} = 20 km, (b) R_{RUP} = 50 km, (c) R_{RUP} = 120 km, and (d) R_{RUP} = 200 km.

where ν is the mean annual rate of the source; $P(IM>im)$ is the probability that the ground motion intensity, IM, exceeds a specified value, im, considering the uncertainties of all the random variables given the occurrence of the earthquake; $P(IM>im|M, R, X_3, \cdots, X_n)$ is the probability that, given a magnitude M, a distance R and other possible random variables $X_3, \cdots, X_n$, the ground motion intensity IM exceeds a specified value im, and n is the number of random variables; $f_M(m)$ represents the probability density function (PDF) of the magnitude occurring in the source; $f_R(r)$ is the PDF used to describe the randomness epicenter locations within the source, $f_{X_3}(x_3)\cdots f_{X_n}(x_n)$ represent the PDFs of other possible variables $X_3, \cdots, X_n$.

Other possible variables include such as the stress drop $\Delta\sigma$, the site diminution κ_0, the mass density of crust ρ, and the shear-wave velocity of the crust β, etc. Although these parameters are often treated as constants in the deterministic estimation of FAS using Equation 1, it can easily be inferred that they inherently have uncertainties. More importantly, when these uncertainties are considered, the V_{eq} varies even for a certain magnitude,

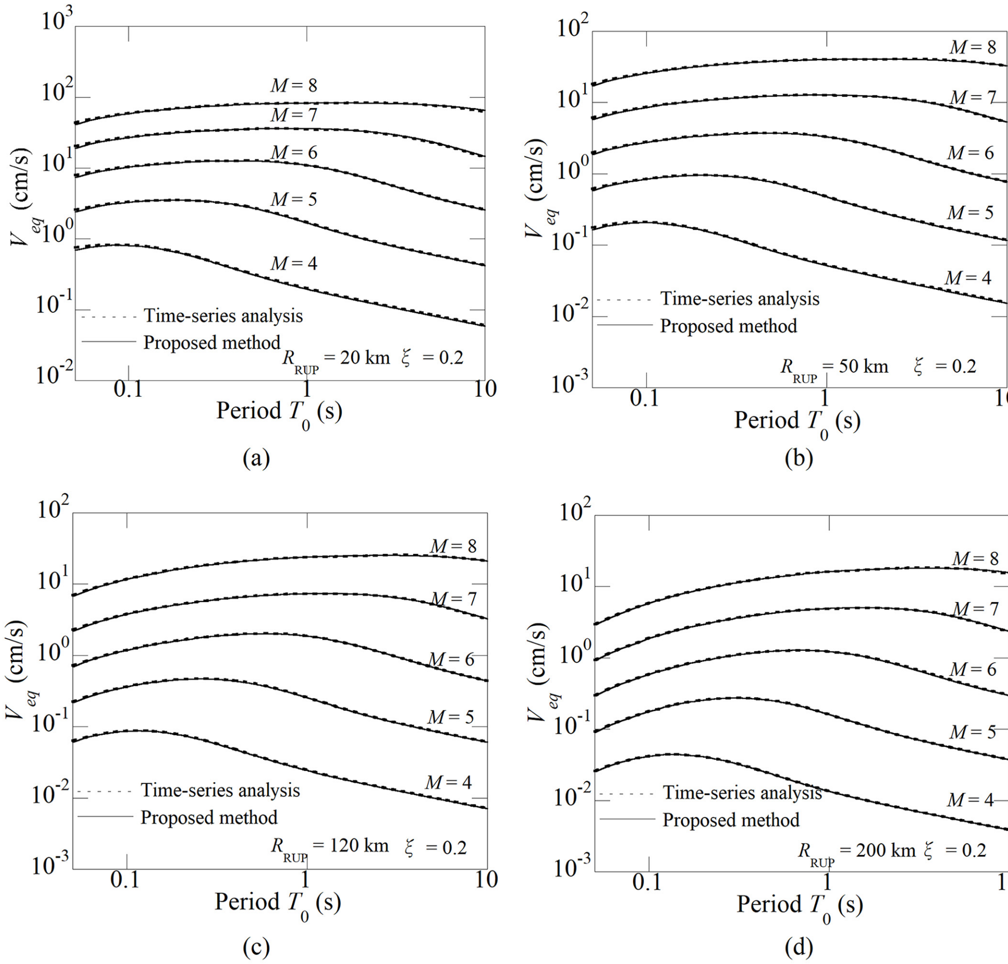

Figure 2. Comparison of V_{eq} results calculated by the proposed method and time-series analysis for a 20% damping ratio considering different moment magnitude M with the rupture distance R_{RUP} being: (a) R_{RUP} = 20 km, (b) R_{RUP} = 50 km, (c) R_{RUP} = 120 km, and (d) R_{RUP} = 200 km.

distance, and site condition, which is consistent with real observation. This phenomenon known as the aleatory uncertainty in traditional GMPE-based PSHA can be reflected to some extent by considering uncertainties of these seismological parameters. Generally, mean values of the site diminution κ_0, the mass density of crust ρ, and the shear-wave velocity of the crust β can be determined for a specific region according to previous studies (Boore, 2015). The mean value of stress drop $\Delta\sigma$ can be determined using a small number of earthquakes with small-to-moderate magnitude (Boore, 2015). Regarding the probability distributions of these seismological parameters, since they have received limited attention so far, they are simply assumed to be lognormal distributions with a certain value of variation coefficient at the current stage. Such an assumption warrants further investigation based on inversion analyses of real seismic records in future studies.

In addition, epistemic uncertainties also should be incorporated into the PSHA, especially in regions with limited ground-motion data. The traditional GMPE-based PSHA

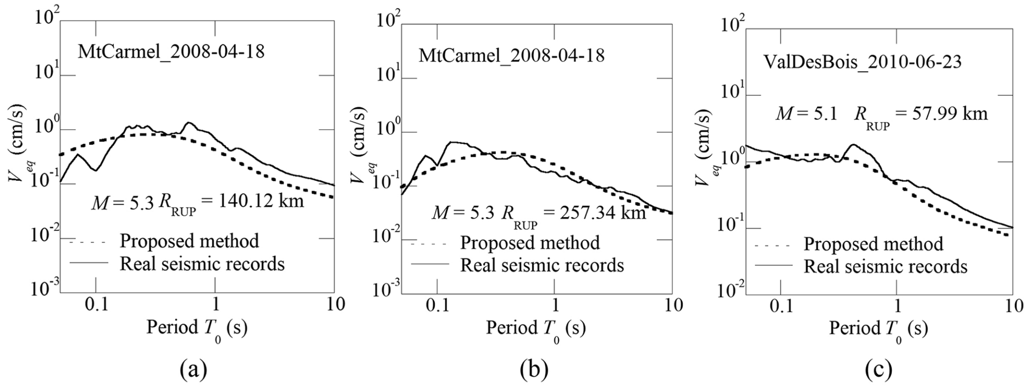

Figure 3. Comparison of V_{eq} results calculated using the proposed method and real seismic records for a 5% damping ratio.

approach addresses epistemic uncertainties typically by employing multiple alternative GMPEs with corresponding weights through a logic tree scheme (Macedo et al., 2020; Tselentis et al., 2010). Then, engineers can address the confidence level based on a set of hazard curves obtained from different GMPEs. In the proposed framework, a similar methodology can be applied to address epistemic uncertainties. Various alternative models for geometric attenuation $Z(R)$ and anelastic attenuation $Q(f)$ in Equation 1 can be applied, with each model assigned weights through a logic tree scheme. The literature review conducted by Boore (2015) reveals that over 40 attenuation models have been developed between 1983 and 2014 for CENA. This number may be significantly fewer than those in regions with abundant data, and epistemic uncertainties in regions with limited ground-motion data may be higher. Nevertheless, with the accumulation of ground-motion data in such regions, more and more reliable attenuation models will be developed, and their application in the proposed framework will lead to more reliable results.

Generally, a theoretical solution for Equation 7 containing multiple integrals can hardly be obtained. Therefore, it is common practice in the traditional PSHA approach using GMPE to discretize the continuous distributions for M and R and convert the integrals into discrete summations (Baker, 2008). Each element within these discrete summations can be treated as an individual earthquake, characterized by magnitude, distance, focal parameters, and so on. Since the natural logarithm of the ground-motion-intensity GMPE, that is, ln IM, is typically considered to follow a normal distribution, the probability that IM exceeds a specified value for each individual earthquake can be directly obtained using the cumulative distribution function (CDF) of the normal distribution. Ultimately, the intensity exceedance rate can be obtained by summing that of each individual earthquake.

However, employing such an approach to compute the annual intensity exceedance rate for the proposed framework using the FAS model is not feasible. The reasons are as follows. (1) Different from the traditional PSHA approach using GMPE, the proposed framework requires additional integral calculations to derive V_{eq} from FAS using Equation 4-1 for each individual earthquake. Moreover, considering that the FAS model involves numerous uncertainty parameters, if their distributions are all discretized, it would necessitate a substantial number of integral calculations using Equation 4-1. (2) More importantly, the FAS obtained from Equation 1 for an individual earthquake is a constant instead of a probability distribution like the traditional GMPE. Therefore, to obtain the intensity exceedance rate, statistical analysis based on a large number of samples is needed. Especially, when a small exceedance probability is of interest, distributions for uncertainty parameters in the FAS model should be discretized with a very small interval. This, in turn, leads to an unacceptable increase in computational costs.

Essentially, the above approach is totally same with the Monte Carlo simulation. Specifically, (1) first, generate enough samples for each random variable following given distributions; (2) then, estimate V_{eq} results according to generated samples for each random variable using the proposed method in Section 2; (3) finally, calculate the exceedance probability $P(IM>im)$ by statistical analysis of all the obtained V_{eq} results. The accuracy of results by the Monte Carlo simulation depends on the number of generated samples for each random variable; it increases with increasing the sample number. We attempted to calculate $P(IM>im)$ using 100,000 samples for each random variable, which is considered a necessary number to obtain a reliable V_{eq} corresponding to a usually used return period of 500 years. However, it costs about 2 h for a single oscillator period considering a single source. If multiple sources and oscillator periods are considered in real cases, the Monte Carlo simulation can hardly be accepted.

Therefore, to simply solve the multiple integrals in Equation 7, an efficient method, namely, the moment method (Zhao and Ono, 2001), is adopted in this paper. The moment method calculates the exceedance probability $P(IM>im)$ by two fundamental steps: (1) assume a distribution form for the ground-motion intensity V_{eq} defined in terms of the first several statistical moments; and (2) estimate the first several statistical moments of the ground motion intensity V_{eq} according to the PDFs of the basic random variables M, R, and $X_3, \cdots, X_n$. The two steps are detailed in the following two sections, respectively.

Cumulative distribution function of V_{eq}

The ground motion intensity V_{eq} is assumed to follow a three-parameter distribution defined in terms of mean value, deviation and skewness (Zhao et al., 2001). The reason for using the three-parameter distribution is that it can better fits statistical data particularly those with skewness than the traditional two-parameter distributions, for example, normal and lognormal distributions. The CDF of the three-parameter distribution, $F(V_{eq})$, is expressed as,

$$F(V_{eq}) = \Phi\left[\frac{1}{\alpha_{3V_{eq}}}\left(\sqrt{9+\frac{1}{2}\alpha_{3V_{eq}}^2+6\alpha_{3V_{eq}}\frac{V_{eq}-\mu_{1V_{eq}}}{\sigma_{V_{eq}}}}-\sqrt{9-\frac{1}{2}\alpha_{3V_{eq}}^2}\right)\right] \tag{8 - 1}$$

where $\mu_{1V_{eq}}$, $\sigma_{V_{eq}}$, and $\alpha_{3V_{eq}}$ are the mean value, standard deviation, and skewness of the ground motion intensity V_{eq}. The standard deviation $\sigma_{V_{eq}}$ and the skewness $\alpha_{3V_{eq}}$ can be estimated by the following equations

$$\sigma_{V_{eq}} = \sqrt{\mu_{2V_{eq}} - \mu_{1V_{eq}}^2} \tag{8 - 2}$$

$$\alpha_{3V_{eq}} = \frac{\mu_{3V_{eq}} - 3\mu_{2V_{eq}}\mu_{1V_{eq}} + 2\mu_{1V_{eq}}^3}{\sigma_{V_{eq}}^3} \tag{8 - 3}$$

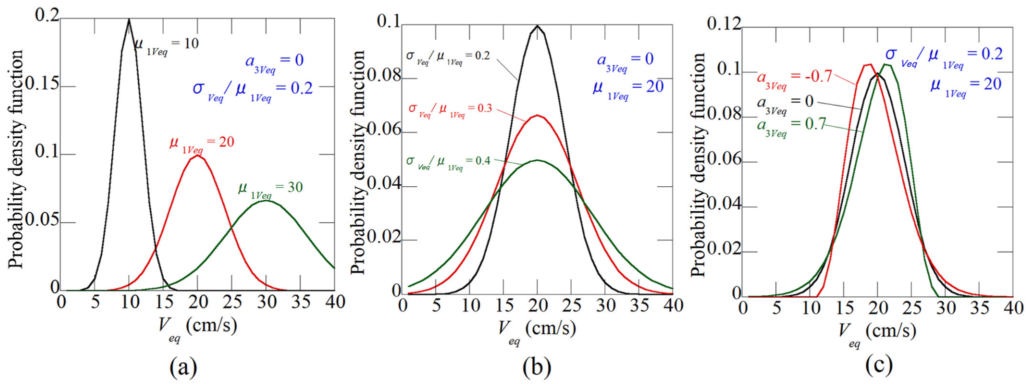

Figure 4. The PDFs of the three-parameter distribution considering different values of (a) the mean value $\mu_{1V_{eq}}$, (b) standard deviation $\sigma_{V_{eq}}$, and (c) skewness $\alpha_{3V_{eq}}$.

where $\mu_{1V_{eq}}$, $\mu_{2V_{eq}}$, and $\mu_{3V_{eq}}$ are the first-order, second-order, and three-order statistical moments of the ground motion intensity V_{eq}, respectively. Figure 4 shows PDFs of the three-parameter distribution considering different values of the mean value $\mu_{1V_{eq}}$, standard deviation $\sigma_{V_{eq}}$, and skewness $\alpha_{3V_{eq}}$.

The first three moments based on the point-estimate method

It can be noted that from Equations 8-1 to 8-3, once the three first three moments, that is, $\mu_{1V_{eq}}$, $\mu_{2V_{eq}}$, and $\mu_{3V_{eq}}$, are obtained, the CDF of the ground motion intensity V_{eq} can be determined, and then, $P(IM>im)$ can be easily obtained. In theory, the kth-order statistical moment $\mu_{kV_{eq}}$ is expressed as,

$$\mu_{kV_{eq}} = E[(V_{eq})^k] = \int\limits_M \int\limits_R \int\limits_{X_3} \cdots \int\limits_{X_n} (V_{eq})^k f_M(m) f_R(r) f_{X_3}(x_3) \cdots f_{X_n}(x_n) dm dr dx_3 \cdots dx_n \tag{9}$$

It can be noted that Equation 9 also contains complex multiple integrals. To simplify the calculation, the point-estimate method (Zhao and Ono, 2000) is adopted. The point-estimate method is always conducted in standard normal space to easily determine the estimating points. The kth-order moment $\mu_{kV_{eq}}$ in standard normal space can be expressed as

$$\mu_{kV_{eq}} = \int \cdots \int (V_{eq}(T^{-1}(\mathbf{U}))^k \varphi(\mathbf{u}) du \tag{10}$$

where $T^{-1}(\mathbf{U}) = \mathbf{X}$ is the inverse normal transformation which can be realized by Rosenblatt transformation (Hohenbichler and Rackwitz, 1981); $\mathbf{X} = [X_1, X_2, X_3, \cdots X_n]$ is a vector of the random variables in original space, X_1 represent the magnitude M, and X_2 represents the distance R; $\mathbf{U} = [U_1, U_2, U_3, \cdots U_n]$ is a vector of standard normal random variables corresponding to $\mathbf{X}$, $\varphi(\mathbf{u})$ is the joint probability density function of $\mathbf{U}$.

Then, applying the point-estimate method in standard normal space, the kth-order moment $\mu_{kV_{eq}}$ can be expressed as,

$$\mu_{kV_{eq}} \cong \sum \left(\prod_{i=1}^{n} P_{di} \right) \left\{ V_{eq} \left[T^{-1}(u_{d1}, u_{d2}, u_{d3}, \cdots, u_{dn}) \right] \right\}^k \tag{11}$$

where d is a combination of n items from a group $[1, 2, \cdots, m]$, m is the number of estimating points, di is the ith item of d, u_{di} is the value of dith estimating point, and P_{di} is the weight corresponding to u_{di}.

Since there are m^n combination of n items from a group $[1, 2, \cdots, m]$, m^n points, that is, m^n times calculation of the ground-motion intensity V_{eq}, will be required for Equation 11. When n and m are large, the computation of Equation 11 also can become excessive. To further simplify the calculation, the bivariate dimension-reduction (Rahman and Xu, 2004) is used here, thus, $\mu_{kV_{eq}}$ can be expressed as,

$$\mu_{kV_{eq}} \cong \sum_{1 \leq i < j \leq n} \mu_{L_2}^k - (n-2) \sum_{i=1}^{n} \mu_{L_1}^k + \frac{(n-1)(n-2)}{2} \mu_{L_0}^k \tag{12 - 1}$$

In Equation 12-1, $\mu_{L_0}^k$ is expressed as

$$\mu_{L_0}^k = \left\{ V_{eq} \left[T^{-1}(0, 0, \cdots, 0) \right] \right\}^k \tag{12 - 2}$$

and $\mu_{L_1}^k$ is one dimensional integral function, which can be approximated as a summation form based on the Gauss-Hermite integration,

$$\mu_{L_1}^k = \int_{-\infty}^{\infty} \left\{ V_{eq} \left[T^{-1}(0, \cdots, u_{ir}, \cdots, 0) \right] \right\}^k \varphi(u_i) du_i = \sum_{r=1}^{m} P_r \left\{ V_{eq} \left[T^{-1}(0, \cdots, u_{ir}, \cdots, 0) \right] \right\}^k \tag{12 - 3}$$

$\mu_{L_2}^k$ is two-dimensional integral function, which also can be approximated as a summation form based on the Gauss-Hermite integration,

$$\begin{aligned} \mu_{L_2}^k &= \int_{-\infty}^{\infty} \int_{-\infty}^{\infty} \left\{ V_{eq} \left[T^{-1}(0, \cdots, u_{ir_1}, \cdots, u_{jr_2} \cdots, 0) \right] \right\}^k \varphi(u_i) \varphi(u_j) du_i du_j \\ &= \sum_{r_1=1}^{m} \sum_{r_2=1}^{m} P_{r_1} P_{r_2} \left\{ V_{eq} \left[T^{-1}(0, \cdots, u_{ir_1}, \cdots, u_{jr_2}, \cdots, 0) \right] \right\}^k \end{aligned} \tag{12 - 4}$$

The estimation points u_{ir}, u_{ir_1}, and u_{jr_2} as well as the corresponding weights P_r, P_{r_1} and P_{r_2} have been well established and can be directly obtained from Zhao and Ono (2000).

Numerical examples

To investigate the validity of the proposed approach, the annual intensity exceedance rates are calculated considering an example point source in this section. The epicentral distance is 30 km, and the focal depth is 20 km. A total of 5 random variables are considered in the analyses, that is, the moment magnitude M, density of crust ρ, stress drop $\Delta\sigma$, shear-wave velocity of crust β, and site diminution κ_0. According to the Guttenberg-Richter relation (Tselentis et al., 2010), the PDF of M is expressed as

$$f_M(m) = \frac{\beta_0 \exp(-\beta_0(m - m_0))}{1 - \exp(-\beta_0(m_{max} - m_0))}, m_0 \leqslant m \leqslant m_{max} \tag{13}$$

m_0 is the minimum threshold magnitude; m_{max} is the maximum threshold magnitude, and $\beta_0 = bln10$, and b is the Guttenberg-Richter's parameter. In the example calculation, m_0 is set as 6, m_{max} is set as 8, and β_0 is set as 2.6. The PDFs of other random variables are assumed and shown in Table 1. For convenient, the mean annual rate of the source ν is considered as 1. The values of other seismological parameters for CENA are used and are determined according to Boore and Thompson (2015).

In addition, a seven-point estimation is adopted in this section, the estimation points and corresponding weights are given by,

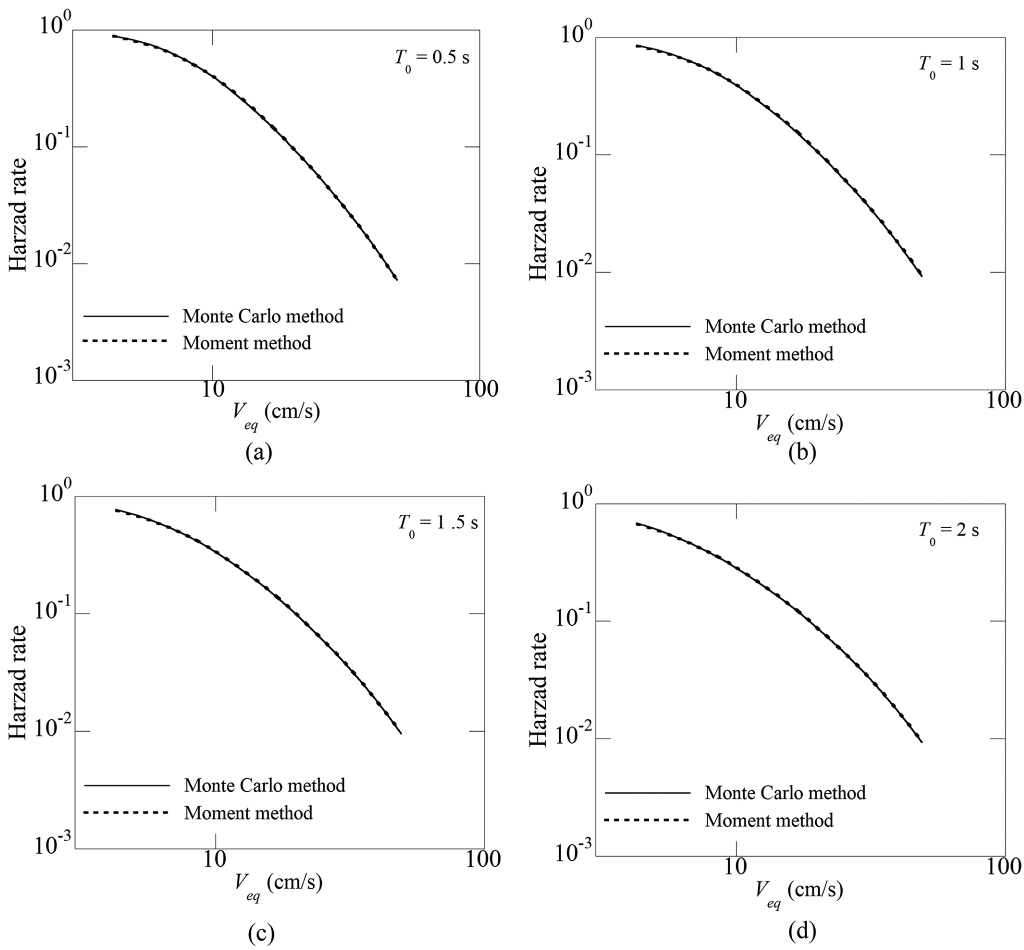

Figure 5. Comparison of the annual intensity exceedance rates calculated by the proposed approach and Monte Carlo simulation for cases with a 5% damping ratio: (a) T_0 = 0.5 s, (b) T_0 = 1.0 s, (c) T_0 = 1.5 s, and (d) T_0 = 2.0 s.

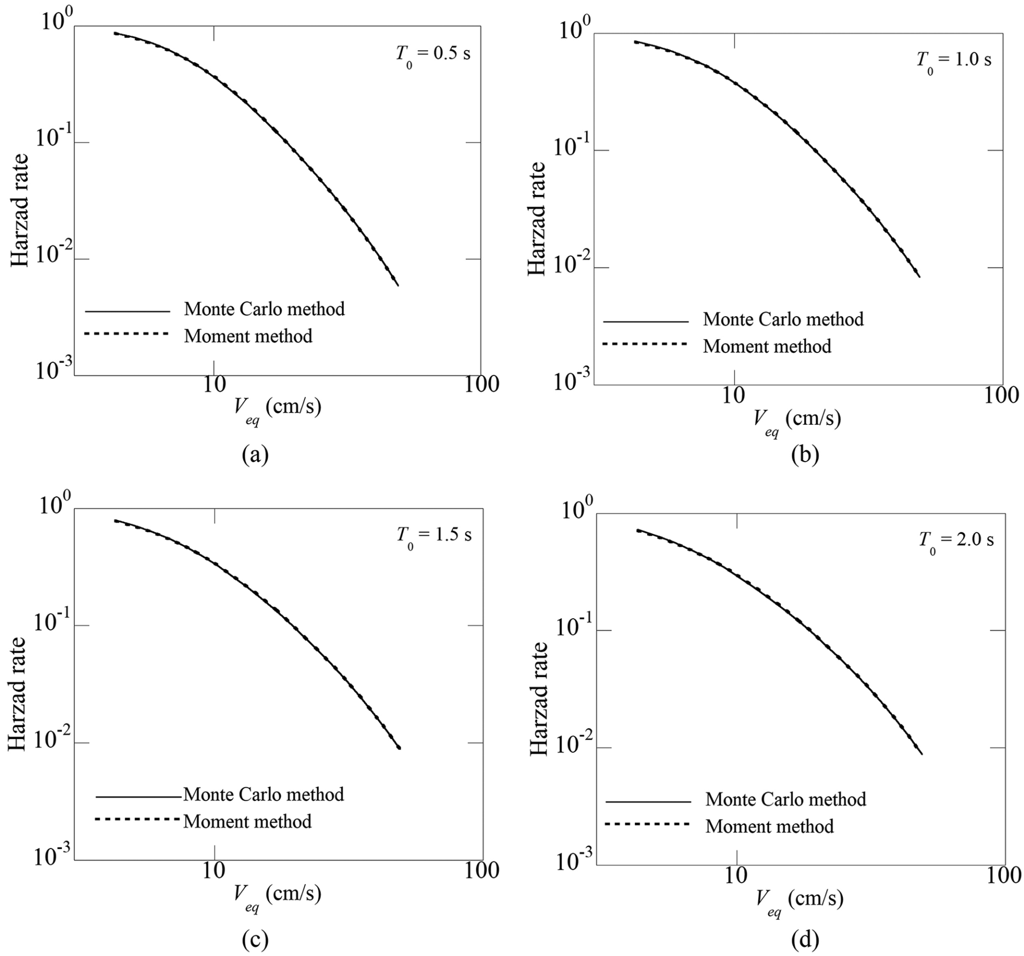

Figure 6. Comparison of the annual intensity exceedance rates calculated by the proposed approach and Monte Carlo simulation for cases with a 20% damping ratio: (a) T_0 = 0.5 s, (b) T_0 = 1.0 s, (c) T_0 = 1.5 s, and (d) T_0 = 2.0 s.

$$\begin{cases} u_{d_1} = -3.7504397 & P_1 = 5.48269\times10^{-4} \\ u_{d_2} = -2.3667594 & P_2 = 3.07571\times10^{-2} \\ u_{d_3} = -1.1544054 & P_3 = 0.2401233 \\ u_{d_4} = 0 & P_4 = 0.4571427 \\ u_{d_5} = 1.1544054 & P_5 = 0.2401233 \\ u_{d_6} = 2.3667594 & P_6 = 3.07571\times10^{-2} \\ u_{d_7} = 3.7504397 & P_7 = 5.48269\times10^{-4} \end{cases} \tag{14}$$

Then, the annual intensity exceedance rates are calculated based on the proposed approach and Monte Carlo simulation. The Monte Carlo simulation uses 100,000 samples for each random variable. Representative results for four oscillator periods are presented in Figures 5 and 6. Figure 5 shows the results of a 5% damping ratio, and Figure 6 shows the results of a 20% damping ratio. It can be noted that the results by proposed approach agree very well with those by the Monte Carlo simulation. Moreover, the proposed method is much more efficient than the Monte Carlo simulation. It only costs about 8 s for a single

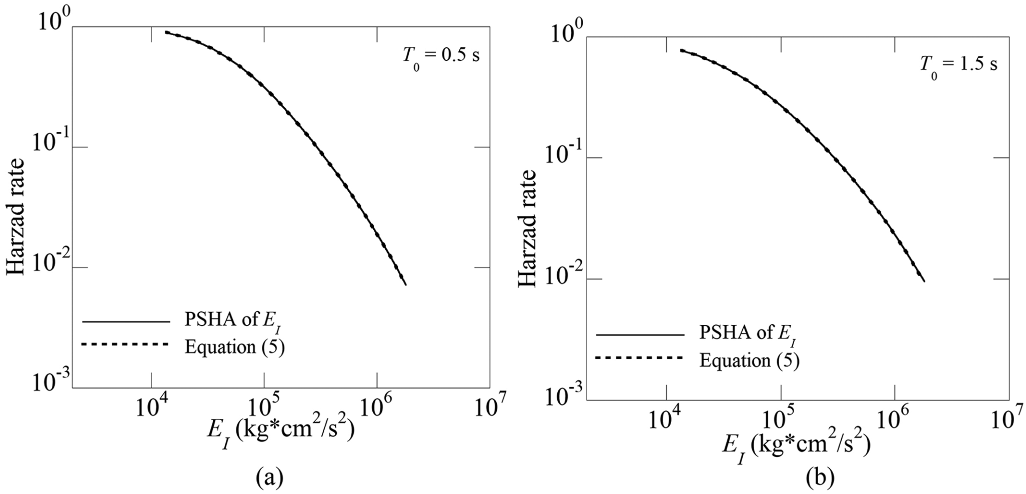

Figure 7. Comparison of the annual exceedance rates of the input energy spectrum E_I calculated based on PSHA and Equation 5 for cases with a 5% damping ratio: (a) T_0 = 0.5 s and (b) T_0 = 1.5 s.

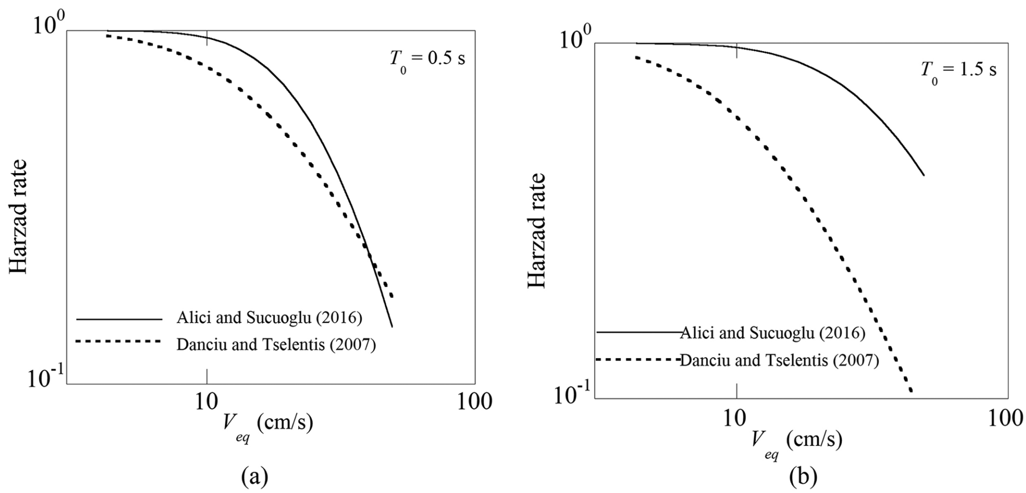

Figure 8. The annual intensity exceedance rates calculated by the traditional GMPE-based approach for cases with a 5% damping ratio: (a) T_0 = 0.5 s and (b) T_0 = 1.5 s.

oscillator period considering a single source, while it costs about 2 h to complete the same calculation using the Monte Carlo simulation. It can also be found that the proposed approach can directly predict hazard curves of V_{eq} for multiple damping ratios.

As for the hazard curve for the input energy spectrum E_I, it can be directly converted from that of the equivalent input energy velocity V_{eq}, using Equation 5. This is because E_I exhibits a monotonically related relationship with V_{eq}, expressed as Equation 5. The probability of exceeding a specific value of V_{eq} is equivalent to the probability of exceeding the corresponding E_I, as calculated by Equation 7. The hazard curves of E_I directly converted from those of V_{eq} are compared with hazard curves of E_I calculated based on PSHA of E_I

using Equations 4-1 and 7, in Figure 7. The PSHA of E_I was conducted using Monte Carlo simulation, with the mass m set as 1500 kg. It can be found that the hazard curves of E_I converted from those of V_{eq} are the same as those calculated based on PSHA. For the estimation of the exceedance probability of a variable not monotonically related to V_{eq}, convolution may be needed, as detailed by Macedo et al. (2020).

Furthermore, annual exceedance rates for V_{eq} are also calculated based on the traditional approach using the GMPE of V_{eq}. To be consistent with the results in Figures 5 and 6, efforts were made to find V_{eq} GMPEs developed using ground motions recorded in CENA. However, no such GMPEs were found, and consequently, two V_{eq} GMPEs for other regions were adopted (Alıcı and Sucuoğlu, 2018; Danciu and Tselentis, 2007). The GMPE of Alıcı and Sucuoğlu (2018) was developed using ground motions in the Next Generation Attenuation project database, which contains records from many countries. The GMPE of Danciu and Tselentis (2007) was developed using ground motions in Greece from the European Strong Motion database. Figure 8 shows the hazard curves calculated based on the traditional approach using the two GMPEs. It can be found that results using the two GMPEs developed using different databases are significantly different. The difference supports that when performing a PSHA for a specific region, using GMPE for V_{eq} from other regions may lead to unreasonable results. Furthermore, the results based on the traditional GMPE-based approach are also very different from those from the proposed method, as seen by comparing Figures 5 and 8. These results indicate that when performing a PSHA at regions lacking strong ground-motion records, the application of GMPEs for V_{eq} from other regions may be unreasonable. Since the FAS model can be determined using a small number of records with small-to-moderate magnitudes (Boore, 2015, 2018, 2020) owing to its linear scaling law, the proposed approach has greater applicability for regions lacking strong ground-motion records.

Conclusion

This study developed a new approach for performing the probabilistic seismic hazard analysis (PSHA) in terms of the input energy spectrum, E_I, in regions lacking ground-motion records. Specifically, a model of Fourier amplitude spectrum (FAS), which can be determined using a small number of seismic records with small-to-moderate magnitudes, is used, and then the E_I of ground motion is obtained based on the relationship between E_I and FAS. Furthermore, an efficient method, namely, the moment method, is applied to calculate the annual intensity exceedance rate. Then, several example calculations are conducted to demonstrate the validity of the proposed framework:

1. The E_I values of ground motion obtained from the FAS model based on the proposed approach agree very well with those acquired from the time-series analysis.
2. The annual intensity exceedance rate calculated by proposed approach agree very well with those by the Monte Carlo simulation.
3. Unlike the conventional PSHA approach, the proposed framework can give E_I values as well as corresponding hazard curves for multiple damping ratios in a straightforward manner.
4. The proposed framework not only is suitable for regions lacking ground-motion records but also performs much more efficiently than using the Monte Carlo simulation in calculating the annual intensity exceedance rate without loss of accuracy.
5. This study primarily focuses on the methodology for PSHA in terms of E_I and V_{eq} in regions lacking ground-motion records. While the proposed approach offers

several methodological advantages, as previously mentioned, its practical implementation currently faces challenges and demands further research in the future. Notably, due to limited research on the probability distributions of seismological parameters, this study relies on certain assumptions. It is anticipated that future studies delving into the probability characteristics of these seismological parameters will enhance the practical applicability of the proposed method.

Declaration of conflicting interests

The author(s) declared no potential conflicts of interest with respect to the research, authorship, and/or publication of this article.

Funding

The author(s) disclosed receipt of the following financial support for the research, authorship, and/or publication of this article: This study was partially supported by the National Natural Science Foundation of China (grant no. 52278135), the authors are grateful for the financial support.

Research data and code availability

The Fourier amplitude spectra and time series used in the analysis were created using the Stochastic-Method SIMulation (SMSIM) programs obtained from http://daveboore.com/software_online.html (accessed 5 March 2024). The seismic ground motion records were downloaded from the Pacific Earthquake Engineering Research Center database at https://ngawest2.berkeley.edu/ (accessed 5 March 2024).

References

Akiyama H (1985) *Earthquake-Resistant Limit-State Design for Buildings*. Tokyo, Japan: University of Tokyo Press.

Akiyama H, Yang ZY and Kitamura H (1993) A proposal of design energy spectra allowing for rock and soil conditions. *Journal of Structural and Construction Engineering (Transactions of AIJ)* 450: 59–69.

Alıcı FS and Sucuoğlu H (2016) Prediction of input energy spectrum: Attenuation models and velocity spectrum scaling. *Earthquake Engineering & Structural Dynamics* 45(13): 2137–2161.

Alıcı FS and Sucuoğlu H (2018) Elastic and inelastic near-fault input energy spectra. *Earthquake Spectra* 34(2): 611–637.

Atkinson GM and Boore DM (2014) The attenuation of Fourier amplitudes for rock sites in eastern North America. *Bulletin of the Seismological Society of America* 104(1): 513–528.

Baker JW (2008) An introduction to probabilistic seismic hazard analysis (PSHA), version 1.3. Available at: https://faeng.ufms.br/files/2019/06/Baker_Introduction_PSHA.pdf (accessed February 1, 2023)

Bayless J and Abrahamson NA (2018) *An empirical model for Fourier amplitude spectra using the NGA-West2 database*. PEER report no. 2018-07, 2 December. Berkeley, CA: Pacific Earthquake Engineering Research Center, University of California, Berkeley.

Beresnev I and Atkinson GM (1998) FINSIM: A FORTRAN program for simulating stochastic acceleration time histories from finite faults. *Seismological Research Letters* 69: 27–32.

Boore DM (2003) Simulation of ground motion using the stochastic method. *Pure and Applied Geophysics* 160: 635–676.

Boore DM (2005) SMSIM—Fortran programs for simulating ground motions from earthquakes (version 2.3): A revision of OFR 96-80-A. Technical report no. 96-80, 15 August. Reston, VA: United States Geological Survey.

Boore DM (2009) Comparing stochastic point-source and finite-source ground-motion simulations: SMSIM and EXSIM. *Bulletin of the Seismological Society of America* 99(6): 3202–3216.

Boore DM (2010) Orientation-independent, nongeometric-mean measures of seismic intensity from two horizontal components of motion. *Bulletin of the Seismological Society of America* 100(4): 1830–1835.

Boore DM (2015, April) *Point-source stochastic-method simulations of ground motions for the PEER NGA-East project, chapter 2 in NGA-East: Median ground-motion models for the Central and Eastern North America region*. PEER report no. 2015/04, pp. 11–49. Berkeley, CA: Pacific Earthquake Engineering Research Center, University of California, Berkeley.

Boore DM (2018) Ground-motion models for very-hard-rock sites in Eastern North America: An update. *Seismological Research Letters* 89(3): 1172–1184.

Boore DM (2020) Revision of Boore (2018) ground-motion predictions for Central and Eastern North America: Path and offset adjustments and extension to 200 m/s $\leqslant$ VS30 $\leqslant$ 3000 m/s. *Seismological Research Letters* 91(2A): 977–991.

Boore DM and Thompson EM (2015) Revisions to some parameters used in stochastic-method simulations of ground motion. *Bulletin of the Seismological Society of America* 105(2A): 1029–1041.

Boore DM, Campbell KW and Atkinson GM (2010) Determination of stress parameters for eight well-recorded earthquakes in Eastern North America. *Bulletin of the Seismological Society of America* 100(4): 1632–1645.

Bora SS, Scherbaum F, Kuehn N and Stafford P (2014) Fourier spectral- and duration models for the generation of response spectra adjustable to different source-, propagation-, and site conditions. *Bulletin of Earthquake Engineering* 12(1): 467–493.

Bora SS, Scherbaum F, Kuehn N and Stafford P (2016) On the Relationship between Fourier and response spectra: Implications for the adjustment of empirical ground-motion prediction equations (GMPEs). *Bulletin of the Seismological Society of America* 106(3): 1235–1253.

Bora SS, Scherbaum F, Kuehn N, Stafford P and Edwards B (2015) Development of a response spectral ground-motion prediction equation (GMPE) for seismic-hazard analysis from empirical Fourier spectral and duration models. *Bulletin of the Seismological Society of America* 105(4): 2192–2218.

Chai YH and Fajfar P (2000) A procedure for estimating input energy spectra for seismic design. *Journal of Earthquake Engineering* 4(4): 539–561.

Chapman MC (1999) On the use of elastic input energy for seismic hazard analysis. *Earthquake Spectra* 15(4): 607–635.

Cheng Y, Lucchini A and Mollaioli F (2014) Proposal of new ground-motion prediction equations for elastic input energy spectra. *Earthquakes and Structures* 7(4): 485–510.

Cheng Y, Lucchini A and Mollaioli F (2020) Ground-motion prediction equations for constant-strength and constant-ductility input energy spectra. *Bulletin of Earthquake Engineering* 18(1): 37–55.

Chou CC and Uang CM (2000) Establishing absorbed energy spectra—An attenuation approach. *Earthquake Engineering & Structural Dynamics* 29(10): 1441–1455.

Danciu L and Tselentis GA (2007) Engineering ground-motion parameters attenuation relationships for Greece. *Bulletin of the Seismological Society of America* 97(1B): 162–183.

Decanini LD and Mollaioli F (1998) Formulation of elastic earthquake input energy spectra. *Earthquake Engineering & Structural Dynamics* 27(12): 1503–1522.

Decanini LD and Mollaioli F (2001) An energy-based methodology for the assessment of seismic demand. *Soil Dynamics and Earthquake Engineering* 21(2): 113–137.

Du B, He Z, Wu Y, Huang G and Pan F (2020) A compatible energy demand estimate considering code-specified design spectra. *Soil Dynamics and Earthquake Engineering* 137(8): 106273.

Gong MS and Xie LL (2005) Study on comparison between absolute and relative input energy spectra and effects of ductility factor. *Acta Seismologica Sinica* 18(6): 717–726.

Goulet CA, Kottke A, Boore DM, Bozorgnia Y, Hollenback J, Kishida T, Der Kiureghian A, Ktenidou OJ, Kuehn NM, Rathje EM, Silva W, Thompson EM and Wang X-Y (2018) Effective amplitude spectrum (EAS) as a metric for ground motion modeling using Fourier amplitudes. In: *Proceedings of the 2018 seismology of the Americas meeting*, Miami, FL, 14–17 May.

Hohenbichler M and Rackwitz R (1981) Non-normal dependent vectors in structural safety. *Journal of the Engineering Mechanics Division: ASCE* 107(6): 1227–1238.

Housner G (1956, June) Limit design of structures to resist earthquakes. In: *Proceedings of the 1st world conference on earthquake engineering*, Berkeley, CA.

Kottke AR and Rathje EM (2013) Comparison of time series and random-vibration theory site-response methods. *Bulletin of the Seismological Society of America* 103(3): 2111–2127.

Kunnath SK and Chai YH (2004) Cumulative damage-based inelastic cyclic demand spectrum. *Earthquake Engineering & Structural Dynamics* 33(4): 499–520.

Kuwamura H and Galambos TV (1989) Earthquake load for structural reliability. Journal of Structural Engineering: ASCE 115(6): 1446–1462.

Kuwamura H, Kirino Y and Akiyama H (1994) Prediction of earthquake energy input from smoothed Fourier amplitude spectrum. *Earthquake Engineering & Structural Dynamics* 23: 1125–1137.

Lavrentiadis G, Abrahamson NA and Kuehn NM (2023) A non-ergodic effective amplitude ground-motion model for California. *Bulletin of Earthquake Engineering* 21: 5233–5264.

Lavrentiadis G and Abrahamson NA (2023) A non-ergodic spectral acceleration ground motion model for California developed with random vibration theory. *Bulletin of Earthquake Engineering* 21: 5265–5291.

Macedo J, Candia G, Lacour M and Liu C (2020) New developments for the performance-based assessment of seismically-induced slope displacements. *Engineering Geology* 277: 105786.

Nigam NC and Jennings PC (1969) Calculation of response spectra from strong-motion earthquake records. *Bulletin of the Seismological Society of America* 59(2): 909–922.

Ordaz M, Huerta B and Reinoso E (2003) Exact computation of input-energy spectra from Fourier amplitude spectra. *Earthquake Engineering & Structural Dynamics* 32(4): 597–605.

Rahman S and Xu H (2004) A univariate dimension-reduction method for multi-dimensional integration in stochastic mechanics. *Probabilistic Engineering Mechanics* 19(4): 393–408.

Rathje EM and Ozbey MC (2006) Site-specific validation of random vibration theory-based seismic site response analysis. *Journal of Geotechnical and Geoenvironmental Engineering* 132(7): 911–922.

Tselentis G-A, Danciu L and Sokos E (2010) Probabilistic seismic hazard assessment in Greece—Part 2: Acceleration response spectra and elastic input energy spectra. *Natural Hazards and Earth System Sciences* 10(1): 41–49.

Vahdani R, Gerami M and Vaseghi-Nia MA (2019) The spectra of relative input energy per unit mass of structure for Iranian earthquakes. *International Journal of Civil Engineering* 17: 1183–1199.

Wang X and Rathje EM (2016) Influence of peak factors on site amplification from random vibration theory based site-response analysis. *Bulletin of the Seismological Society of America* 106(4): 1733–1746.

Zhang HZ and Zhao YG (2020) Damping modification factor based on random vibration theory using a source-based ground-motion model. *Soil Dynamics and Earthquake Engineering* 136: 106225.

Zhang HZ and Zhao YG (2021) Effects of earthquake magnitude, distance, and site conditions on spectral and pseudospectral velocity relationship. *Bulletin of the Seismological Society of America* 111(6): 3160–3174.

Zhang HZ and Zhao YG (2022) Damping modification factor of acceleration response spectrum considering seismological effects. *Journal of Earthquake Engineering* 26(16): 8359–8382.

Zhang HZ, Zhao YG, Ge FW, Fang YC and Ochiai T (2023a) Estimation of input energy spectrum from pseudo-velocity response spectrum incorporating the influences of magnitude, distance, and site conditions. *Engineering Structures* 274: 115165.

Zhang HZ, Zhao YG, Ochiai T and Fang YC (2023b) Relationship between SDOF-input-energy and Fourier amplitude spectral amplification ratios. *Bulletin of the Seismological Society of America* 113(3): 1230–1247.

Zhang R, Zhao YG and Zhang HZ (2023c) An efficient method for probability prediction of peak ground acceleration using Fourier amplitude spectral model. *Journal of Earthquake Engineering* 28: 1495–1511.

Zhao YG and Ono T (2000) New point estimates for probability moments. *Journal of Engineering Mechanics: ASCE* 126(4): 433–436.

Zhao YG and Ono T (2001) Moment methods for structural reliability. *Structural Safety* 23(1): 47–75.

Zhao YG, Ono T, Idota H and Hirano T (2001) A three-parameter distribution used for structural reliability evaluation. *Journal of Structural and Construction Engineering ((Transactions of AIJ)* 66(546): 31–38.

Zhao YG, Zhang R and Zhang HZ (2023) Probabilistic prediction of ground-motion intensity for regions lacking strong ground-motion records. *Soil Dynamics and Earthquake Engineering* 165: 107706.